

the combined unfavorable effects of both propeller and yawing initiated the left-wing stall at about  $\alpha = 10$  deg, for the case of positive  $\beta$  (+10 deg). This corresponds to a left-turn situation as described above, resulting in a left yawing moment (into the turn) accompanied by a very high rolling moment extending beyond the control limits of the airplane.<sup>6</sup> The stall of the right wing is initiated only at above  $\alpha = 13$  deg (Fig. 3) and the negative rolling moments are then reduced.

Because of the dihedral of the test airplane wing (5 deg), rolling moments on the order of  $\pm 0.01$  for both yaw conditions are measured at the lower angles of attack ( $\alpha < 9$  deg in Fig. 3). On the other hand, because of the presence of the fuselage (the test aircraft had a low wing), the trailing half-wing section has a higher tendency to stall (in spite of the lower effective angle of attack). The combination of this effect with the propeller slipstream results in the considerable difference between the positive and negative yawing as shown in Fig. 3. That is, when yawing the aircraft to the right, the resulting rolling moment is within control limits, whereas, yawing it to left will bring the aircraft beyond its control limits.

### Concluding Remarks

The study of propeller effect reported here shows that for a typical single-engine, low-wing, general-aviation aircraft with untapered wings, the propeller upwash on the left wing initiated separation at an angle of attack which is 3 deg smaller than the angle of attack at which the separation of the right wing occurred. When the aircraft was yawed, it was found that positive yaw angles resulted in a violent rolling moment and wing separation was initiated at smaller angle of attack. For the negative yaw condition, the separation occurred at 2–3 deg of angle of attack later, and the resulting rolling moments were within control limits. The above finding suggests that aircraft similar to the one tested, under positive sideslip condition, are likely to face a stall-spin entry when performing, for example, a low-speed final left turn with excessive rudder deflection before landing.

### Acknowledgment

This work was done while the first author held an NRC Senior Research Associateship at NASA Ames Research Center.

### References

- 1 "Special Study: General Aviation Stall/Spin Accidents 1967–1969," Rept. NTSB-AAS-72-8, National Transportation Safety Board, Sept. 1972.
- 2 Anderson, S.B., "Historical Overview of Stall/Spin Characteristics of General Aviation Aircraft," *Journal of Aircraft*, Vol. 16 July 1979, pp. 455–461.
- 3 Kroeger, R.A. and Feistel, T.W., "Reduction of Stall-Spin Entry Tendencies Through Wing Aerodynamic Design," SAE Paper 760481, presented at the Business Aircraft Meeting, Wichita, Kansas, April 1976.
- 4 DiCarlo, D.J. and Johnson, J.L. Jr., "Exploratory Study of the Influence of Wing Leading-Edge Modification on the Spin Characteristics of a Low-Wing Single-Engine General Aviation Airplane," AIAA Paper 79-1837, Aug. 1979.
- 5 Winkelmann, A.E., Barlow, J.B., Saini, J.K., Anderson, J.D. Jr., and Jones, E., "The Effects of Leading Edge Modifications on the Post Stall Characteristics of Wings," AIAA Paper 80-0199, 1980.
- 6 Feistel, T.W., Anderson, S.B., and Kroeger, R.A., "Alleviation of Spin-Entry Tendencies Through Localization of Wing-Flow Separation," *Journal of Aircraft*, Vol. 18, Feb. 1981, pp. 69–75.
- 7 Sweberg, H.H. and Dingeldein, R.C., "Summary of Measurements in Langley Full Scale Tunnel of Maximum Lift Coefficients and Stalling Characteristics of Airplanes," NACA Rept. 829, 1945.
- 8 Fink, M.P., Freeman, D.C. Jr., and Greer, H.D., "Full-Scale Wind-Tunnel Investigation of the Static Longitudinal and Lateral Characteristics of a Light Single-Engine Airplane," NASA TN D-5700, March 1970.
- 9 Shivers, J.P., Fink, M.P., and Wave, G.M., "Full-Scale Wind-Tunnel Investigation of the Static Longitudinal and Lateral Characteristics of a Light Single-Engine Low-Wing Airplane," NASA TN D-5857, June 1970.

## Applications of Similitude in Airship Design

C. K. Lavan\* and C. K. Drummond†  
Goodyear Aerospace Corporation, Akron, Ohio

### Introduction

THE Buckingham  $\pi$  theorem is often thought of simply as a tool for the reduction of the number of independent variables required in an experimental study of natural phenomena. Similitude is, therefore, often overlooked during the conceptual phase of engineering design. This Note describes two clarifications gained by implementing the Buckingham  $\pi$  theorem in a conceptual airship design study. First, a volume sensitivity parameter is obtained that permits a very close description of traditional airship performance characteristics in terms of a single curve. Second, the appropriate parameters for nondimensionalization of drag for an airship is discussed.

### Airship Volume Sensitivity

The necessary airship volume  $V$  for a prescribed mission depends on the airship's altitude  $z$ , velocity  $U$ , payload  $W$ , and endurance  $t$ . Only three basic dimensions—mass, length, and time—are necessary to express the five variables dimensionally. Interpreting air density  $\rho$  to correspond to the effect of altitude on the airship performance, the functional relationship for the airship volume is

$$F(V, \rho, U, W, t) = 0 \quad (1)$$

The  $\pi$  theorem states that the number of variables ( $n=5$ ) minus the number of dimensions ( $r=3$ ) is equal to the number of independent parameters ( $n-r=2$ ) that characterize the problem. Classic dimensional analysis<sup>1</sup> leads one readily to find the two  $\pi$  parameters:

$$\pi_1 = V/U^3 t^3 \quad (2)$$

$$\pi_2 = W/\rho U^4 t^2 = W/(\rho U^2)(Ut)^2 \quad (3)$$

Note the significance of the second term, which can be interpreted as the ratio of the useful load to the product of the dynamic pressure and the ferry range squared. From the  $\pi$  theorem,

$$F(\pi_1, \pi_2) = 0 \quad (4)$$

from which we define a new function,  $f$ , such that

$$\pi_1 = f(\pi_2)$$

so that a general relationship for airship volume is

$$\frac{V}{U^3 t^3} = f\left(\frac{W}{\rho U^4 t^2}\right)$$

Received June 10, 1986; revision received Jan. 20, 1987. Copyright © American Institute of Aeronautics and Astronautics, Inc., 1987. All rights reserved.

\*Engineer Specialist, Naval Airship Division. Member AIAA.

†Senior Development Engineer, Naval Airship Division. Member AIAA.

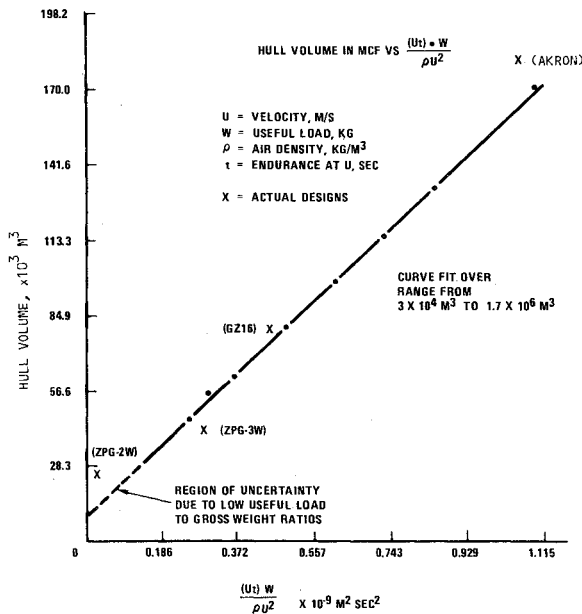


Fig. 1 Hull volume sensitivity analysis.

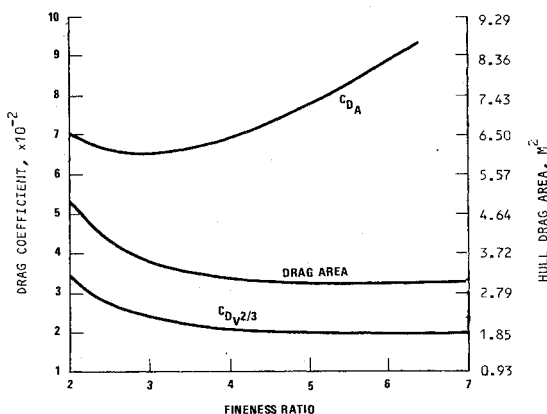


Fig. 2 Bare hull drag coefficient and drag area for a baseline 56,600 m<sup>3</sup> airship volume.

Recognizing the rules governing the manipulation of  $\pi$  parameters,<sup>1</sup> we simplify the analysis by assuming a constant of proportionality,  $C_1$ , for the function described by  $f$ ; the expression for airship volume is now

$$V = C_1 (U t) (W / \rho U^2) \quad (5)$$

In words, we expect the hull volume to increase with increasing ferry range, increasing payload, and decreasing dynamic pressure (increasing altitude).

An interactive computer program—the Goodyear Airship Synthesis Program (GASP)—was used to generate data to check the dependence of volume (in the 30,000–170,000-m<sup>3</sup> range) on the sensitivity parameter in Eq. (5). A plot of this data is shown in Fig. 1. Verification of the general trend is provided by a plot of some historical data for airships such as the ZPG-3W.

Figure 1 is a comprehensive measure of the hull volume sensitivity to basic airship design parameters; it provides more succinctly the message of the set of Normand equations discussed by Burgess.<sup>2</sup>

### Nondimensionalization of Airship Drag

Once an optimal airship volume has been established, it is logical to design the hull for minimum drag. Allow the airship volume to be included in the description for drag given by

$$F(D, V, L, R, \nu, \rho, U) = 0 \quad (6)$$

where  $L$  is the theoretical airship length,  $R$  the airship radius, and  $\nu$  the kinematic viscosity of air. Four  $\pi$  parameters are anticipated since there are seven parameters expressible in terms of three basic dimensions; in the situation in which  $V$ ,  $\rho$ , and  $U$  have been selected as the repeating variables,

$$\pi_1 = D / \rho U^2 V^{2/3} \quad (7)$$

$$\pi_2 = L / V^{1/3} \quad (8)$$

$$\pi_3 = R / V^{1/3} \quad (9)$$

$$\pi_4 = \nu / U V^{1/3} \quad (10)$$

the idea is now that

$$\frac{D}{\rho U^2 V^{2/3}} = f \left\{ \frac{L}{V^{1/3}}, \frac{R}{V^{1/3}}, \frac{\nu}{U V^{1/3}} \right\} \quad (11)$$

where the effect of selecting volume as a repeating variable is quite evident. Appreciating that we are at liberty to invert  $\pi$  parameters, the fineness ratio  $\lambda = L/2R$  can be introduced and the functional dependence for drag given by

$$C_D = \frac{D}{\frac{1}{2} \rho U^2 V^{2/3}} = f(\lambda, Re) \quad (12)$$

where the Reynolds number  $Re$  is based on the characteristic length  $V^{1/3}$ . Subject to the conditions described above, Eq. (12) indicates that the appropriate (constant volume airship) reference area for nondimensionalization is  $V^{2/3}$ .

Of importance here is that for an airship of fixed volume and a given Reynolds number, a parametric analysis to establish the fineness ratio for which the drag coefficient is minimized depends on the reference area used. Von Mises<sup>3</sup> remarks that minimizing the resistance of, for instance, a nacelle requires the optimization of fineness ratio for streamlined body of thickness  $t$ , while in airship design the problem is to determine the fineness ratio of a streamlined body of volume  $V$ . Although it might be intuitively deduced that the appropriate characteristic reference area for the airship drag coefficient is  $V^{2/3}$ , dimensional analysis is capable of predicting the same. Physically, the drag area ( $C_D A$ ) will not change for any given reference area; however, minimum airship hull drag area will correspond to minimum drag coefficient when the latter is based on  $V^{2/3}$  rather than  $\pi R^2$ . Figure 2 illustrates this effect for a bare airship hull, where the minimum of  $C_D$  based on  $\pi R^2$  near a fineness ratio of 2.8 corresponds to the results of Ref. 4; when  $C_D$  is based on  $V^{2/3}$ , the minimum is at approximately 6.2 and corresponds with the minimum drag area.

### Conclusion

The utility of dimensional analysis should not be overlooked in the conceptual phase of engineering design. Two different uses of dimensional analysis have been used in the present work. First, the derivation of an airship volume sensitivity parameter eliminates the need for a multitude of single-parameter plots. Second, the  $V^{2/3}$  reference area yielded an airship drag area minimum corresponding to the minimum drag coefficient.

### References

- <sup>1</sup>Murphy, G., *Similitude in Engineering*, Ronald, New York, 1950, pp. 35–40.
- <sup>2</sup>Burgess, C. P., *Airship Design*, Ronald, New York, 1927, pp. 12–35.
- <sup>3</sup>VonMises, R., *Theory of Flight*, Dover, New York, 1959, pp. 102–103.
- <sup>4</sup>Meyers, J., Holm, C., and McAllister, R. (eds.), *Handbook of Ocean Engineering*, McGraw-Hill, New York, 1969, pp. 2–26.